



European Commission's 7th Framework Programme Grant Agreement No. **226520**

Project acronym: **COMBINE**

Project full title: Comprehensive Modelling of the Earth System for Better Climate Prediction and Projection

Instrument: Collaborative Project & Large-scale Integrating Project

Theme 6: Environment Area 6.1.1.4: Future Climate

ENV.2008.1.1.4.1: New components in Earth System modelling for better climate projections

Start date of project: 1 May 2009 Duration: 48 Months

Deliverable Reference Number and Title: D4.1: Preliminary validation of AOGCMs including new sea ice representation

Lead work package for this deliverable: WP4

Organization name of lead contractor for this deliverable: UCL

Due date of deliverable: 31 October 2011 (delayed to 31 March 2012)

Actual submission date: 24 April 2012

Project co-funded by the European Commission within the Seven Framework Programme (2007-2013)		
Dissemination Level		
PU	Public	х
PP	Restricted to other programme participants (including the Commission Services)	
RE	Restricted to a group specified by the consortium (including the Commission Services)	
CO	Confidential, only for members of the Consortium (including the Commission Services)	

1. Introduction

One of the objectives of WP4 of COMBINE was to develop new components in sea ice models and to improve the coupling of sea ice with atmosphere and ocean in three atmosphere-ocean general circulation models (AOGCMs): CNRM-CM5, EC-EARTH and IPSL-CM5. The two concerned sea ice models are GELATO and the Louvain-la-Neuve sea ice model (LIM). The focus was on (i) incorporating processes into those models to better represent the ice categories that are the most fragile and/or (ii) accounting for further processes at the ice-atmosphere interface, e.g., surface melt ponds and snow processes. Here, we report on the developments carried out so far and on their validation in both uncoupled and coupled modes.

2. CNRM contribution

2.1 The original CNRM-CM5.1 AOGCM (CMIP5 model)

GELATO5 is the sea ice component of CNRM-CM5.1 (see Voldoire et al. (2012) for a description of CNRM-CM5.1 and GELATO5, or http://www.cnrm.meteo.fr/gmgec/spip.php?article86 for more details about GELATO). This sea ice model has the following characteristics:

- explicit subgrid-scale ice thickness distribution (four ice categories resolved within each grid cell);
- nine ice layers and one snow layer along the vertical direction;
- prognostic bulk sea ice salinity (Vancoppenolle et al., 2009); temperature- and salinity-dependent sea ice thermal conductivity and specific heat;
- new snow albedo scheme and ocean-ice heat flux parameterization (Schmidt et al., 2004);
- elastic-viscous-plastic rheology; incremental remapping advection; rafting and ridging of ice floes.

The horizontal resolution of GELATO5 is about 1° in the Arctic Ocean. All centennial climate simulations performed within CMIP5 at MF-CNRM (9000 model years) and all decadal climate simulations conducted at CERFACS (3000 years) were carried out with this model.

2.2 Recent developments

2.2.1 Salt and water conservation

The conservation of salt and water in GELATO5 and the coupling procedure between the ocean component of the Nucleous for European Modeling of the Ocean (NEMO) and GELATO5 were significantly improved. More precisely, for the latter point, instead of treating both freshwater input/evaporation and seawater salinity concentration/dilution due to salt exchanges between sea ice and the surface ocean as virtual fluxes, two fluxes were introduced: a freshwater flux and a salt flux. This work was done in close collaboration with IPSL/LOCEAN. As a result, the global mean ocean salinity now drifts by only -3×10^{-4} psu/century in the new coupled model CNRM-CM5.2, compared to -0.011 psu/century in CNRM-CM5.1. The major difference between CNRM-CM5.2 and CNRM-CM5.1 lies in these adjustments, and the possibility to easily activate a surface melt pond parameterization.

2.2.2 Melt ponds

A melt pond parameterization has been incorporated into GELATO5. This parameterization has been validated in both forced and coupled modes.

The parameterization is based on the semi-empirical melt pond scheme included in CICE4, as described in Holland et al. (2011). The melt pond volume (i.e., the product of the pond fraction by the pond depth) is calculated as a state variable. It grows through the addition of a fraction of melting snow, top surface ice ablation and rain. During fall, the pond refreezing (i.e., the formation of an ice lid over the pond) is simulated using a surface heat budget. The pond fraction and depth are derived from the pond volume through a simple linear relationship fitted from field campaign data (SHEBA). The albedo of the melt pond is a function of the pond depth following Ebert and Curry (1993). The pond volume is advected as a volume tracer.

In forced mode, the ocean—sea ice component of CNRM-CM5.2, NEMO-GELATO5, is driven with prescribed atmospheric data derived from the ERA-Interim reanalysis over the period 1990-2009. A correction in air humidity and temperature, based on Lüpkes et al. (2010), is applied. The ice surface albedo compares relatively well with field measurements taken during the SHEBA campaign (Fig.1).

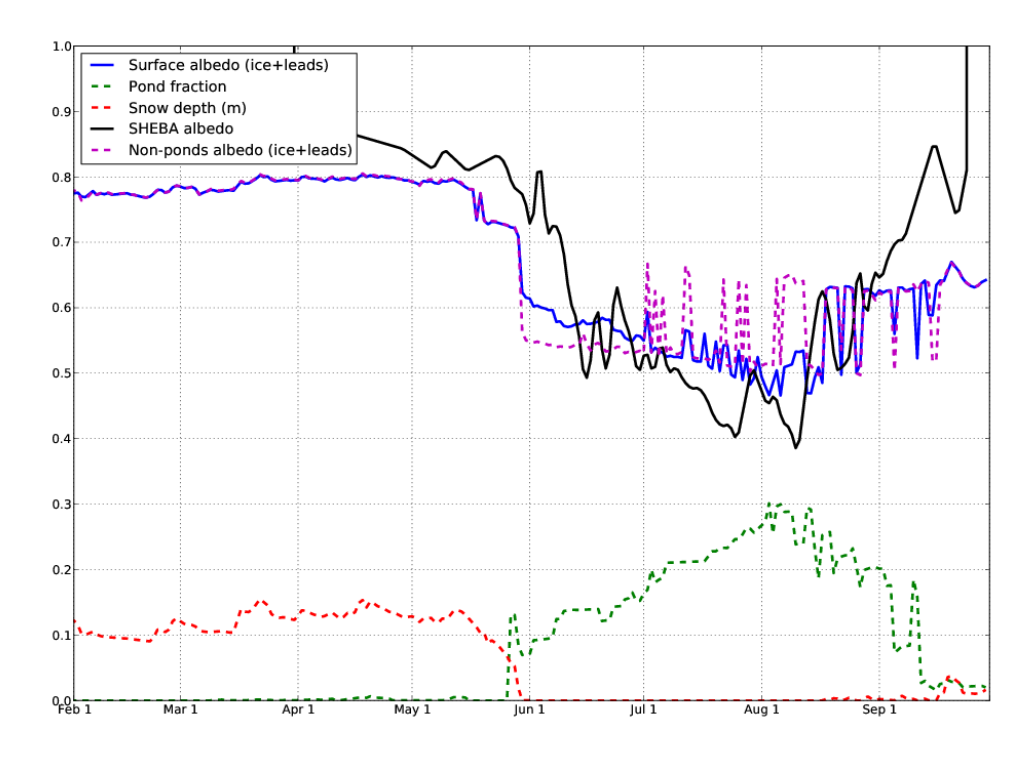


Figure 1: Ice+lead albedo, pond fraction and snow depth (m) modeled by NEMO-GELATO5 during the 1998 winter-spring-summer at SHEBA locations (plotted in blue, green and red, respectively). For comparison, the ice+lead albedo simulated by the same model but without melt pond parameterization is plotted in purple.

2.3 Coupled experiments with CNRM-CM5.2

2.3.1 Experimental design

We ran the following preindustrial experiments with CNRM-CM5.2:

- standard version of the model (including salinity and water conservation corrections);
- same as previous, except that the melt pond scheme was activated.

For both experiments, the ocean was initially at rest. The three-dimensional potential temperature and salinity fields were initialized from Levitus' data. Sea ice was initialized from a state obtained in a previous preindustrial coupled experiment (year 401 of the CMIP5 preindustrial experiment, i.e., the starting point of historical experiments, member 1). The model was spun up for 20 years. This time is clearly too short to allow the deep ocean to reach an equilibrium. However, the surface ocean and sea ice are stable enough to analyse differences between the two experiments over years 21-30. These simulations are also compared to years 401-410 of the CMIP5 preindustrial experiment run with CNRM-CM5.1. When run without explicit melt pond scheme, CNRM-CM5.1 and CNRM-CM5.2 assume that the melting ponded ice albedo is 0.56. This value was found to be optimal from a set of NEMO-GELATO5 experiments forced with ERA-Interim.

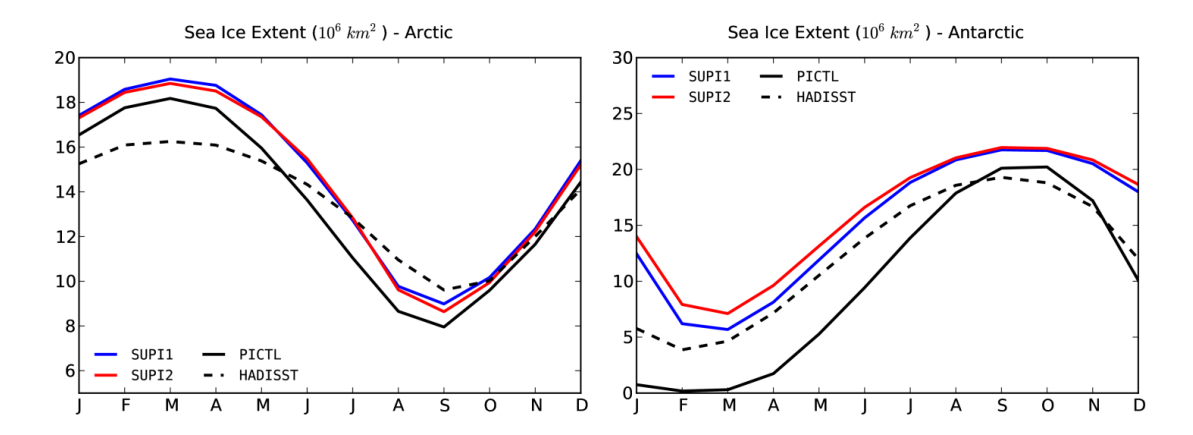


Figure 2: (Left) Mean seasonal cycle of Arctic sea ice extent (in million km²): CMIP5 control run (black, solid line), CNRM-CM5.2 simulations with and without melt pond scheme (blue and red curves, respectively). HadISST data for 1980-1989 are depicted by the dashed line. (Right) Same for the Antarctic.

2.3.2 Results

The mean seasonal cycles of sea ice extent from CNRM-CM5.2 with and without melt pond scheme are compared with those from CNRM-CM5.1 in Fig. 2. The HadISST data over 1980-1989 are also plotted for comparison. We chose not to use the HadISST data for 1870-1879, even if the coupled experiments are run under preindustrial forcings, since those data are probably unrealistic in the Southern Ocean area over this time-span.

The differences between the two experiments carried out with CNRM-CM5.2 are generally weak. We speculate that larger differences would arise under current or future climate forcing. The simulated amplitude of the seasonal cycle of the Arctic sea

ice extent is still overestimated by CNRM-CM5.2. CNRM-CM5.2 is slightly more realistic in summer, but the winter bias is enhanced. Like for CNRM-CM5.1, most of this error is due to an excess of sea ice in the North Pacific (which does not appear in ERA-Interim forced simulations) and, to a lesser extent, by too extensive a sea ice cover in the Norwegian Sea. Fig. 3 shows that the modeled sea ice is more than 0.50 m thinner in the western Arctic in January and July if the melt pond parameterization is activated. Fig. 4 indicates that the albedo of bare sea ice during July is slightly lower if melt ponds are taken into account. Such a parameterization is expected to increase the modeled sensitivity of sea ice.

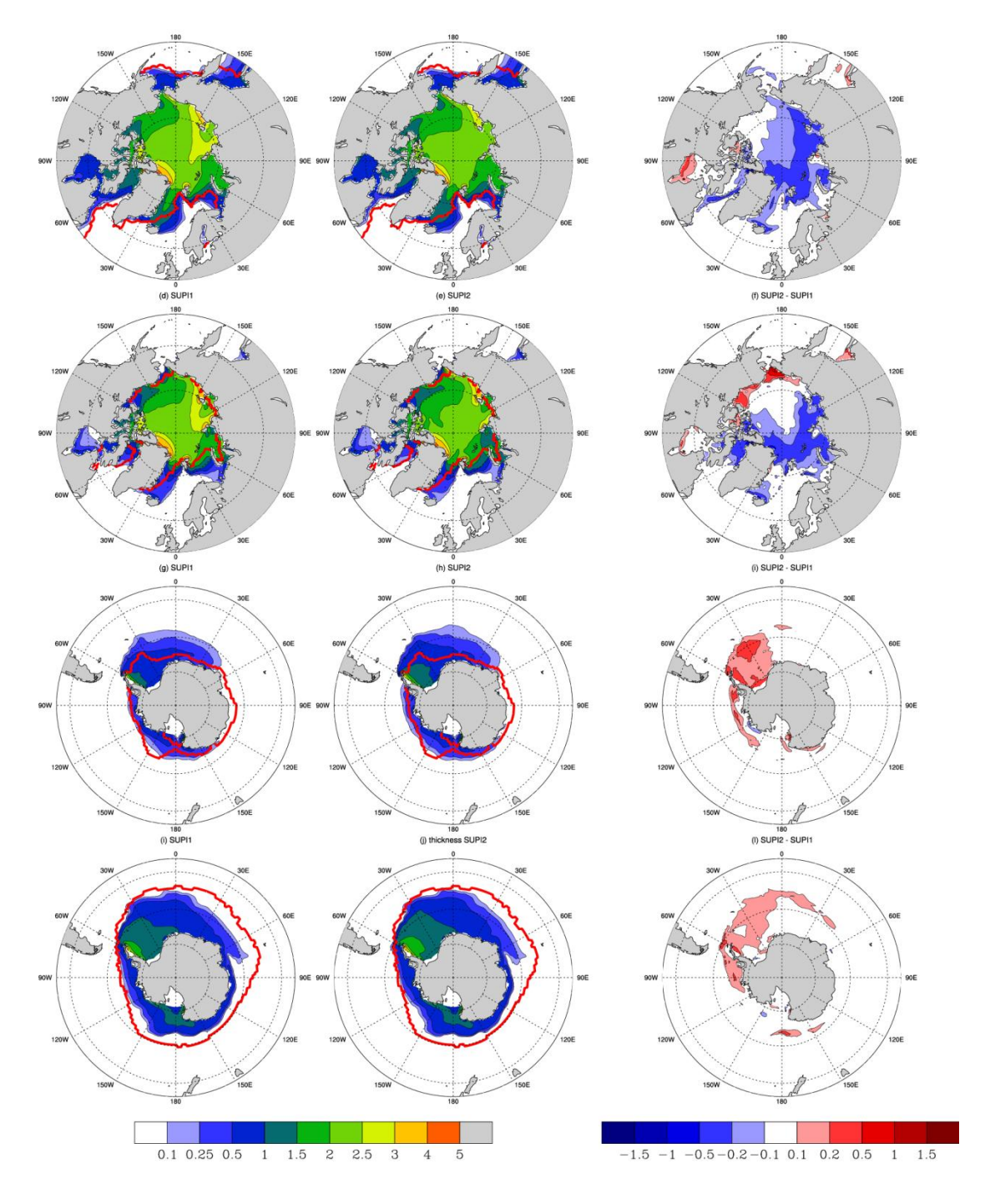


Figure 3: Left, middle and right columns: sea ice thicknesses modeled by CNRM-CM5.2 without explicit melt ponds, with explicit melt ponds and difference (with melt

ponds minus without melt ponds), respectively. First and second rows: January and July in the Arctic, respectively. Third and fourth rows: January and July in the Antarctic, respectively. Units are meters.

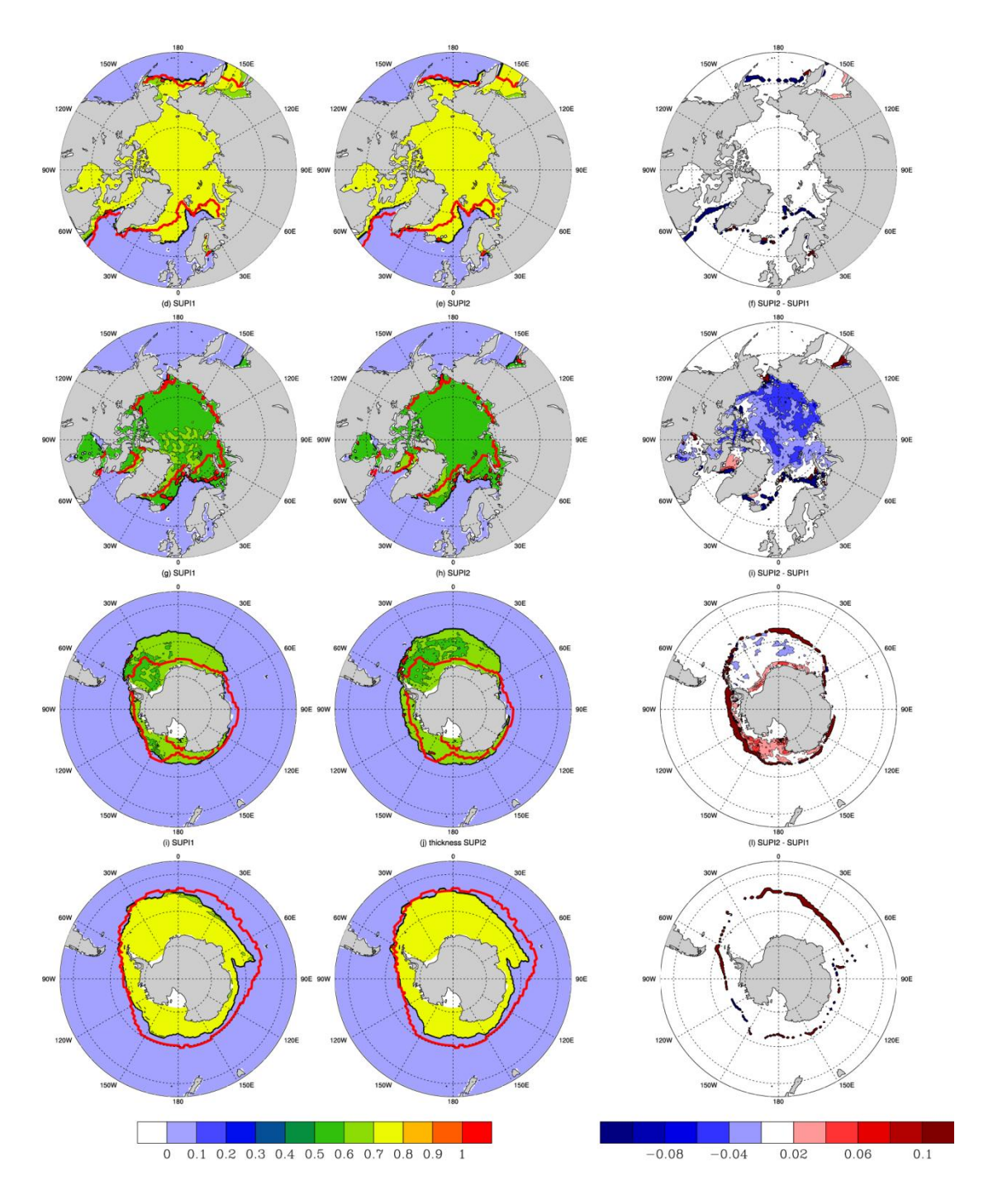


Figure 4: Left, middle and right columns: sea ice albedo (0-1) modeled by CNRM-CM5.2 without explicit melt ponds, with explicit melt pond and difference (with melt ponds minus without melt ponds), respectively. First and second rows: January and July in the Arctic, respectively. Third and fourth rows: January and July in the Antarctic, respectively.

By contrast, the simulation of sea ice is much improved in the Antarctic, particularly in winter. In CNRM-CM5.1, sea ice disappears completely in February and March. This is now corrected in CNRM-CM5.2, highlighting the paramount importance of water and salt conservation for the simulation of Antarctic sea ice. However, the extent of sea ice appears significantly overestimated in December and January. This is confirmed by looking at the sea ice thickness field in Fig. 3. Contrary to the Arctic, the melt pond parameterization tends to produce thicker ice in January and July, particularly in the Weddell, Amundsen and Bellingshausen Seas. This is actually not very surprising since (i) this parameterization was tuned for the central Arctic, where multiyear ice prevails, and (ii) it computes the volume of melt ponds from the amount of surface meltwater, but the fraction/depth of ponds is determined in an empirical way, and implies to make hypotheses on the roughness of sea ice. For example, if melt ponds form on underformed ice (i.e., the sea ice surface is rather flat), one would expect that melt ponds can potentially cover a large fraction of the ice surface, but remain shallow. On the contrary, if the ice surface is very rough, melt ponds will probably be deeper but will cover a smaller fraction of the ice.

These simulations are preliminary – only a transient simulation until 2011 will allow us to fully validate the model results against recent observations.

3. UCL-CNRS contribution

The contribution of UCL covers three main topics:

- 1) the comparison of the output from sea ice models to observations;
- 2) the implementation of new parameterizations of snow processes and wave-ice interactions in LIM3, the latest version of LIM (Vancoppenolle et al., 2009);
- 3) the coupling of sea ice and atmospheric components in climate models in the case where the sea ice model is multi-category, as LIM3 (LIM3 is the standard sea ice component of NEMO (Madec, 2008)).

3.1 Validation of NEMO-LIM3

There is considerable spread in projections of future characteristics of Arctic and Antarctic sea ice as simulated by current AOGCMs. This scatter can be explained by the differences in resolution, initial conditions and sophistication of ocean, atmosphere and sea ice physics in each AOGCM.

Massonnet et al. (2011) isolated the role of sea ice physics in two hindcast simulations (1983-2007) conducted with the ocean—sea ice models NEMO-LIM2 and NEMO-LIM3 at a horizontal resolution of ~1°, driven by the daily NCEP/NCAR reanalysis surface air temperatures and wind speeds. The two experiments only differed in the nature of their sea ice module: LIM2 is a dynamic-thermodynamic sea ice model with a virtual sea ice thickness distribution, a rather simple formulation of heat storage by brine pockets and a viscous-plastic (VP) constitutive law for sea ice rheology; LIM3 is a multi-category ice thickness, enthalpy and age distribution model that explicitly accounts for the vertical distribution of brine into sea ice and uses the advanced elastic-viscous-plastic (EVP) rheology. To address the sensitivity of the sea ice cover to the different model versions, a set of comprehensive metrics for sea ice was developed. Different variables (sea ice concentration, thickness, drift and extent) were evaluated with respect to available observations. We focused both on the mean state and interannual variability of the simulated properties.

The conclusions of this work are hemisphere-dependent (Massonnet et al., 2011). In the Arctic, LIM3 is outperforming LIM2, probably because of (1) its explicit sea ice thickness distribution, allowing a more realistic response to the atmospheric forcing, and (2) the presence of an explicit salinity distribution in sea ice, whose impacts have shown to be significant in previous studies. The conclusions are not as clear in terms of Antarctic sea ice. No model is systematically better than the other one, and for the same metrics, the skills are in general lower than in the Northern Hemisphere (NH). Some limiting factors seem to mask the potential improvement that should come with a more comprehensive sea ice model, such as (1) the quite coarse (~1°) resolution of the ocean model, that does not explicitly represent eddy-related processes despite their importance in the Southern Ocean, (2) the poor quality of atmospheric reanalyses, compared to the NH, and (3) the fact that sea ice is thinner in the Southern Hemisphere (SH), implying that the sea ice cover might be less sensitive to sea ice-related thermodynamic and dynamic processes.

3.2. New physical developments in LIM3

3.2.1. A representation of wave-ice interactions implemented in NEMO-LIM3

Sea ice frequently forms in wavy waters. Penetrating waves break the ice, while the ice attenuates the waves. Swell has been reported up to a few hundred kilometers within the ice cover. Because of ocean waves, young ice floes take a rounded shape that led hungry early explorers to give them the name of pancake ice. Pancake ice seems to grow faster than ice forming in quiet seas.

Based on the fact that wave-ice interactions are not represented in current large-scale sea ice models, the aim of this piece of work was to introduce into NEMO-LIM3 a basic representation of the impact of ocean waves on new ice growth, and to evaluate the importance of pancake ice growth for the large-scale sea ice mass balance.

In order to represent pancake ice in the large-scale ocean—sea ice model NEMO-LIM3 (Vancoppenolle et al., 2009), we proceed in three steps: (i) detection of the ice edge based on the simulated ice concentration using the ERA-40 wave climatology (Sterl and Caires, 2005); (ii) propagation of waves from the ice edge into the ice pack using exponential attenuation; (iii) computation of new ice thickness as a function of wave amplitude in sea ice (Dai et al., unpublished).

Results suggest that wave-ice interactions have a large-scale impact mostly in the SH. In the NH, their influence is rather limited, as the zones where ocean swell is in contact with the ice restrict to a few peripheral seas, namely the Greenland, Okhotsk and Bering Seas.

In the Southern Ocean, the effect of wave-ice interactions as parameterized is to increase the annual mean ice volume (Fig. 5), as the formulation assumes initially thicker ice produced from the freezing of open water. This larger volume implies more ice remaining after summer melt, and therefore a larger summer ice extent. The parameterization also assumes that new ice forms with smaller coverage. Thus, a larger ice extent is found in the simulation with pancake ice than in the control run.

Both the significant impact of wave-ice interactions on the simulated sea ice characteristics and the sensitivity of those to the wave-ice interaction parameters

(wave attenuation, maximum forming ice thickness) suggest that further studies aiming at constraining the wave-ice interactions are necessary.

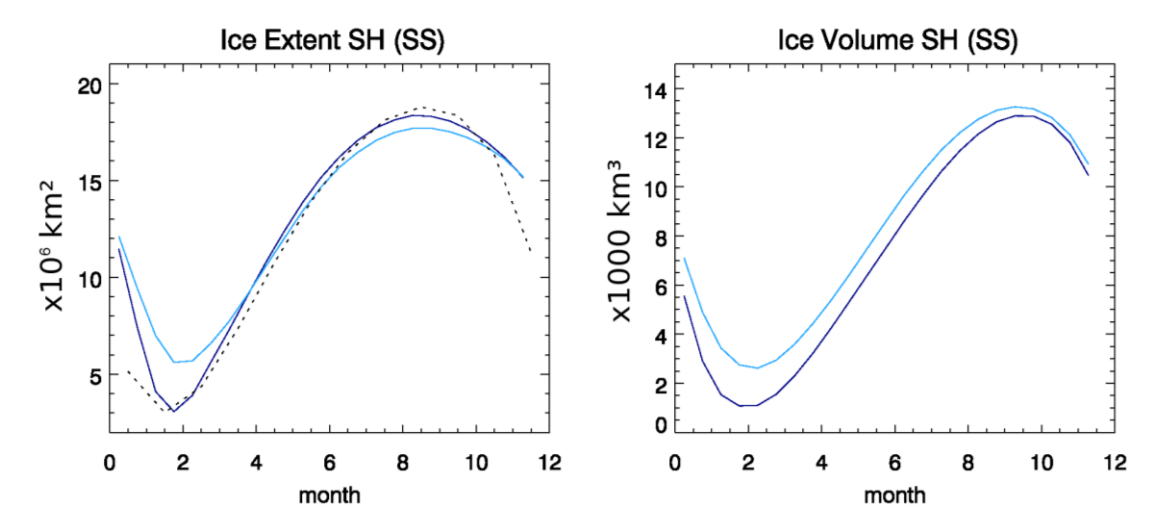


Figure 5: Average 1983-2011 simulated seasonal cycles of (a) sea ice extent and (b) volume in the SH for a run without (dark blue) and with (light blue) pancake ice formation. Observations (Sea Ice Index, www.nsidc.org) are depicted by the dotted line.

3.2.2 Improvement of the snow component of NEMO-LIM3

LIM3 initially had a simple snow representation including only one snow layer with constant physical properties. Since the beginning of COMBINE, a new snow component was implemented in the model. This scheme is multi-layer, with time and space varying snow density and thermal conductivity, and allows for the surface and internal melting of snow, snow ice production and penetration of solar radiation into the snow pack. In addition to the snow thinning process by melt, evaporation of snow in case of low air specific humidity is enabled.

The validation of this new scheme was first done in a one-dimensional framework (Lecomte et. al., 2011) by comparing snow temperature profiles and thickness of the snow/ice system in the model to data sampled at Point Barrow (Alaska) and on the ISPOL floe (Western Weddell Sea, Southern Ocean). The performance of the model was also compared to that of the former representation of snow in LIM3.

The new snow scheme was then incorporated into the full three-dimensional version of NEMO-LIM3, using three snow layers in the dynamic component with a refined stratigraphy in the thermodynamic routines of the model. Because LIM3 is quite sensitive to snow thermal conductivity, the snow component final validation was done by assessing the results from the model using several thermal conductivity parameterizations as functions of density and/or wind speed. Fig. 6 illustrates the mean seasonal cycles of sea ice extent in the NH and SH over 1979-2007 (run performed on a ~1°-resolution horizontal grid) using the best of these parameterizations with respect to observations (from EUMETSAT OSISAF, 2010). A paper presenting this study is in preparation and will be submitted soon for publication.

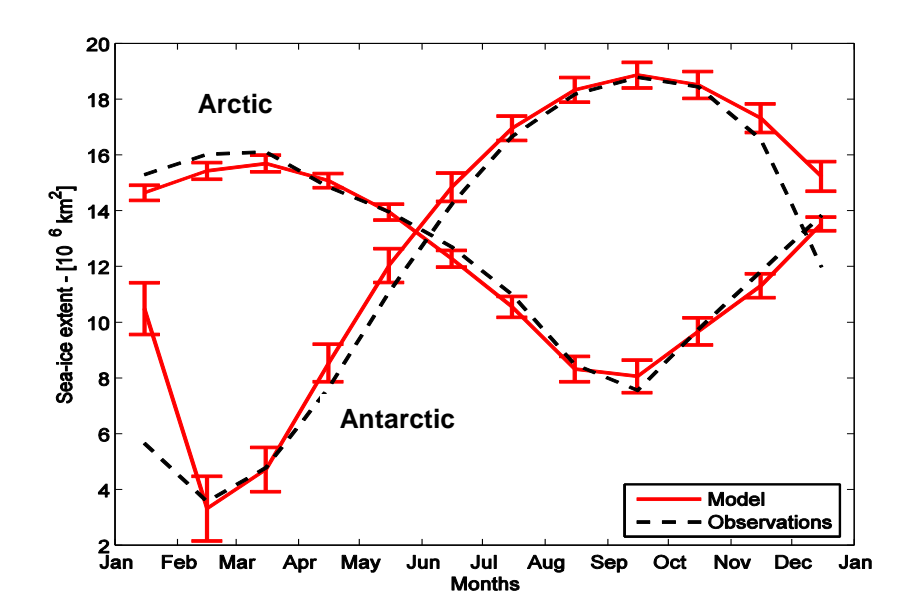


Figure 6: NEMO-LIM3 mean seasonal cycles of sea ice extent in the NH and SH over 1979-2007. Horizontal resolution for the run is \sim 1°. The error bar represents the standard deviation (over 1979-2007) of sea ice extent for each month.

3.3 The coupling of multi-category sea ice models with an atmospheric component

The coupling of new generation sea ice models, including LIM3, with atmospheric models raise new technical problems that have to be addressed for a proper simulation of sea ice characteristics.

The mass balance of sea ice is largely driven by the energy budget at the ice-ocean interface (Maykut and Untersteiner, 1971). Both radiative and turbulent atmospheric heat fluxes to the sea ice are intrinsically coupled to the sea ice surface temperature (SIST): any change in heat flux affects the SIST, which itself determines the magnitude of the atmospheric heat fluxes.

The first generation of sea ice models, including LIM2 (Fichefet and Morales Maqueda, 1997), represented sea ice in a grid cell with a single thickness and area (mono-category). More recent models, including LIM3 (Vancoppenolle et al., 2009), represent sea ice in each grid cell as made of several categories. Each category is characterized by a specific thickness and area. This strategy has been prposed by Thorndike et al. (1975) because (i) ice thickness can vary between roughly 0 and 20 m over subkilometric distances, and (ii) strong variations in surface temperature and net heat flux are found between thin and thick ice (Maykut, 1986).

This multi-category approach raises technical issues for the sea ice—atmosphere coupling in climate models. Ideally, an atmospheric model should enable to compute an energetic balance for each thickness category, which is feasible for atmospheric models enabling sub-surfaces ("tiling"). However, many atmospheric models do not provide this possibility and the way the atmosphere—sea ice heat flux is redistributed among the ice categories may strongly affect the sea ice mass balance. The atmospheric component of the French AOGCM IPSL-CM5 is one of those atmospheric models. Therefore, we decided to investigate how to best redistribute the atmosphere—sea ice heat flux among the ice categories.

A distributor for atmospheric heat fluxes was developed. The simplest distributor is to prescribe the same atmospheric heat flux to each ice category. However, this approach leads to potential problems, as the surface flux depends non-linearly on the ice thickness and the surface state. Thus, we propose a more complex approach, based on the linearization of the non-solar heat flux based on the difference of the category value of SIST with the category-weighted mean SIST. This new flux distributor was tested in forced mode using a pseudo-coupler (section 3.3.1) to validate our approach, and then tested in the framework of a coupled climate model (section 3.3.2).

3.3.1 Simulations in forced mode using a pseudo-coupler

The pseudo-coupler approach aims at emulating the behavior of an atmospheric model without carrying all the technical difficulties to run it. We assume that the atmospheric model is not able to "see" the ice thickness categories, e.g., is able to compute only one series of fluxes for each model grid cell. The coupler used in climate models is an interface module sending the SIST and the ice concentration to the atmosphere, and sending back the atmospheric heat flux F. We emulate the coupler (pseudo-coupler) by using the forcing module of NEMO-LIM3 fed by the category-weighted average of SIST and albedo, and the total ice concentration to compute one single flux F. The flux distributor is part of the ice code that (i) computes the category-dependent fluxes F_l (where l is the category index), using a functional form that warrants energy conservation.

In order to assess the performance of the pseudo-coupler, we performed three simulations. The first one is a control run (hereafter referred as CTL) with NEMO-LIM3 on the ~2° ORCA2 grid over 1979-2007, using the best available computation of the atmospheric heat fluxes: the forcing module of NEMO-LIM3 calculates the atmospheric heat fluxes for each category F_l , using the surface temperature of each category T_l^{su} . Then, two simulations were carried out in the pseudo-coupled configuration: PC+ (with the flux distributor) and PC- (without the flux distributor). PC+ has category-dependent fluxes ($F_l \neq F$), while PC- has the same fluxes over each ice thickness category ($F_l = F$).

Let us first look at the seasonal cycle of sea ice extent in both the NH and SH (Fig. 7). In the two hemispheres, CTL and PC+ are rather similar, while PC- is quite different, with a summer low bias of about 2×10^6 km². The differences in extent are associated with differences in ice volume.

Now, in terms of ice volume (Fig. 8), PC+ slightly underestimates the CTL run values in the NH, with a bias of about 1×10^3 km³. The underestimation of ice volume in PC- is much larger, going up to 10×10^3 km³, and is quasi constant throughout the year. In the SH, the difference between CTL and PC- simulations is much lower (up to 1×10^3 km³) and occurs only during summer. Sea ice volumes for CTL and PC+ are very similar. The difference observed between the NH and SH might be due to the fact that, in the SH, the contribution of thicker ice categories to the ice volume is quasi nil.

Analysis reveals that the flux distributor allows capturing the intensified winter heat loss over thin ice, which promotes more intense and more realistic ice growth, and prevents spurious loss of ice in summer. With only one flux, the ice growth rate in the thinnest ice category is too mild, the ice is resultingly too thin and retreats too far

polewards in summer. This gives reasonable confidence in the ability of the flux distributor to approximate the distribution of the non-solar heat fluxes over the different ice categories.

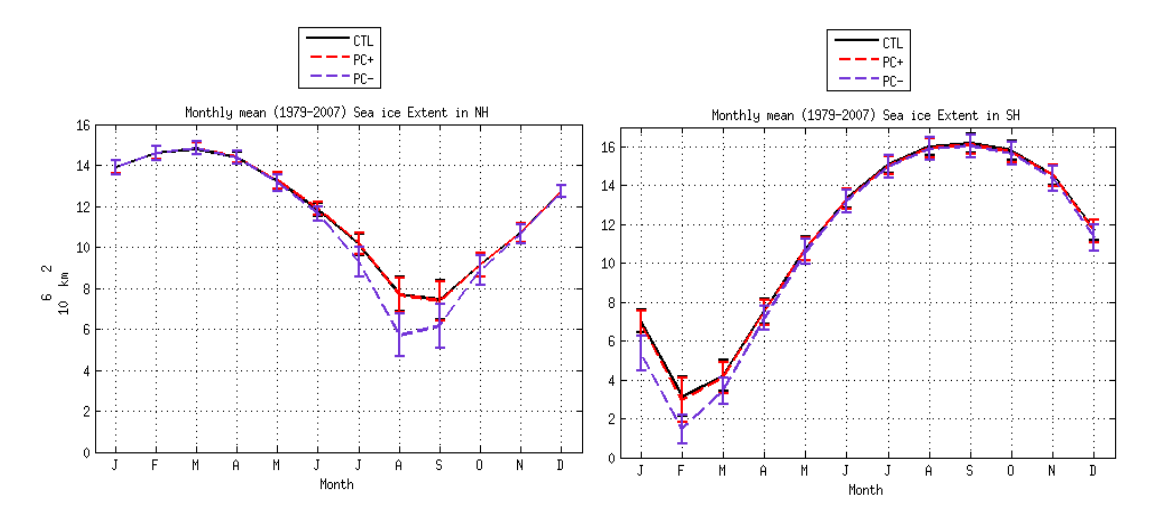


Figure 7: Mean seasonal cycles of sea ice extent in the NH (left) and SH (right) over 1979-2007 for CTL (black lines), PC+ (red lines) and PC- (purple lines) simulations. The error bars denote the $\pm 1\sigma$ deviation of monthly extents during the same period.

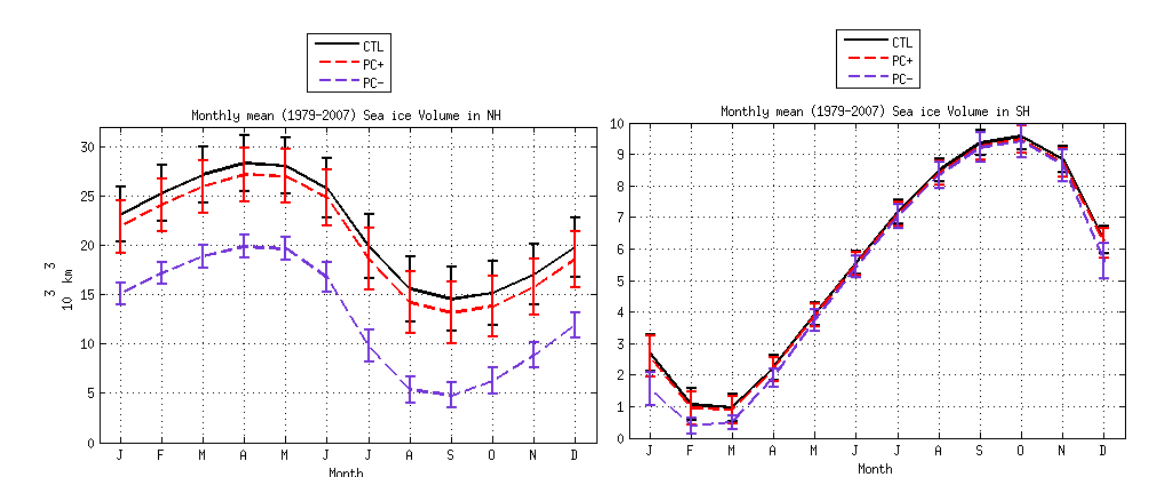


Figure 8: Mean seasonal cycles of sea ice volume in the NH (left) and SH (right) over 1979-2007 for CTL (black lines), PC+ (red lines) and PC- (purple lines) simulations. The error bars represent the $\pm 1\sigma$ deviation of monthly volumes during the same period.

3.3.2 Using the flux distributor in a coupled Earth system model

We coupled the atmospheric component of the AOGCM IPSL-CM5 to the ocean—sea ice model NEMO-LIM3 using the flux distributor. Our main concern was to confirm the results obtained in forced configuration.

We then ran a coupled preindustrial control simulation (CPL) with the new model. The greenhouse gas concentrations, aerosols and solar forcing at the top of the atmosphere were the climatological averages of 1960-1990. Only the last year of the

eight years of simulation was used to compute the mean seasonal cycles of sea ice extent in the NH and SH (Fig. 9).

The preliminary results indicate a good seasonal shape of the sea ice extent, but LIM3 yields too much ice in general compared to a similar coupled run (CTL) conducted with the older version of the sea ice model (LIM2). The overestimation ranges between 3×10^6 km² and 4.5×10^6 km² in the NH, and between 2×10^6 km² and 6×10^6 km² in the SH. In the NH, the maximum and minimum sea ice extents of CPL are shifted compared to CTL. CPL presents a minimum in August and a maximum in January, while in CTL, they occur in September and March, respectively. In the SH, CPL catches the February minimum but has a maximum in August, instead of September in CTL.

This preliminary analysis reveals that the IPSL-CM5/NEMO-LIM3 coupling is running, but the results are not yet satisfactory. Further experiments will be performed in the near future to understand the causes of the noticed biases.

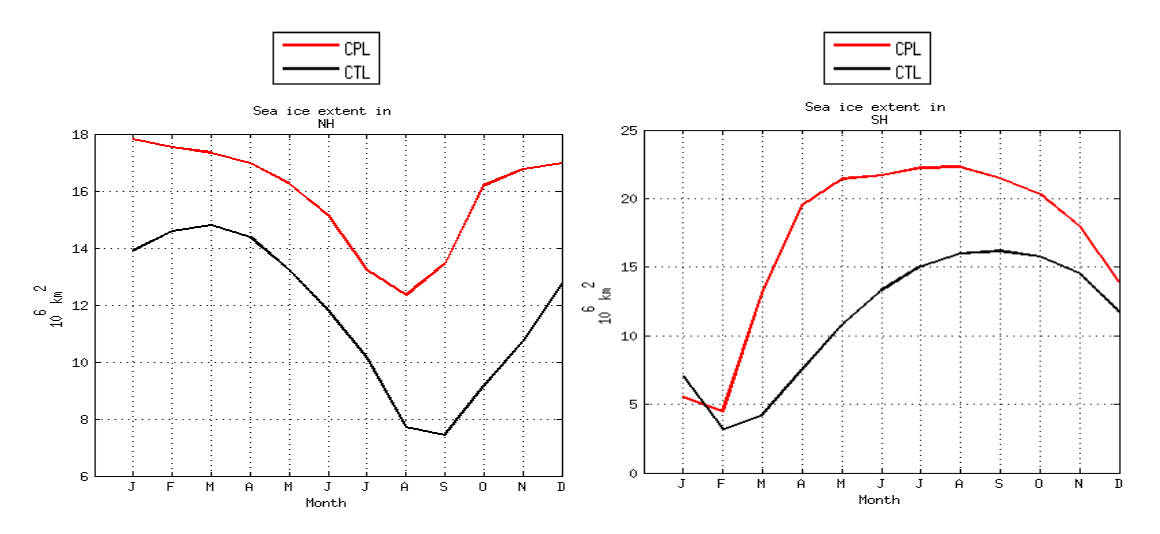


Figure 9: Mean seasonal cycles of sea ice extent in the NH (left) and SH (right) for the CPL and CTL simulations.

4. SMHI Contribution

4.1 New sea ice model for EC-EARTH

Version 3 of EC-EARTH includes NEMO version 3.3.1 as ocean component. This NEMO version came with both LIM2 and LIM3 sea ice models. However, the LIM3 version was not fully implemented for coupled models because the coupling interface only supported LIM2. The coupling interface had to be modified to enable LIM3 to properly interact with the rest of the model. Special attention had to be paid to the multiple sea ice categories in LIM3. The fluxes from the atmosphere to the sea ice (e.g., heat fluxes, precipitation) are computed in the atmosphere and sent to the sea ice model, while the sea ice model sends back state variables (e.g., surface temperature, sea ice fraction). The atmospheric component of EC-EARTH (IFS) has only one single sea ice tile, while LIM3 can have several sea ice categories. Aggregating sea ice variables from various categories before sending them to the atmosphere is straightforward, but distributing the flux from a single tile to multiple sea ice

categories poses a challenge (see Section 3.3). As a first approximation, we simply used the same energy and water fluxes for all sea ice categories, except for the solar flux that we modulate with the albedos of the different ice categories.

4.1.1 Experiments

The new sea ice model was tested in 25-year experiments with the fully coupled EC-EARTH model. The climate forcing – aerosols, greenhouse gases, insolation – is always from year 2000 representing present-day conditions. In all experiments, the ocean starts from Levitus' climatology because EC-EARTH has not been spun-up previously. We can expect some initial adjustments (spin-up) after the initialization and the model will not have reached equilibrium after 25 years. The results presented here should therefore be considered as preliminary. Longer spin-up runs under both present-day and pre-industrial forcing conditions will be carried out once the model tuning will be completed.

EC-EARTH was set up in 3 different configurations for the sea ice component: LIM2, LIM3 with 5 sea ice categories (LIM3/5) and LIM3 with a single sea ice category (LIM3/1). The LIM2 configuration was chosen for comparison because (1) it is still the standard sea ice model in NEMO and (2) it was used in EC-EARTH v2 for CMIP5 experiments. The ocean grid was ORCA1 with 46 vertical levels. The resolution in the atmosphere was T255/N128 with 62 vertical levels. The atmosphere and ocean models interacted every 3 hours through the OASIS-3 coupler.

4.1.2 Results

A 20-year time series of sea ice area is shown in Fig.10. The trend, especially in the SH, reveals that the model has not reached equilibrium yet. Nevertheless, we can already draw few conclusions. In LIM3/5, all ice in the Arctic disappears during summer and reappears in winter. The seasonal cycle in LIM3/5 is much larger than in LIM3/1 or LIM2. The reason for the too strong variability of LIM3/5 is the coupling of the non-solar flux. We assumed that the non-solar heat flux is equal for all sea ice categories, but apparently this assumption leads to a strong thinning of the ice (see Fig. 11), and all ice disappears in the summer season. The model is still cold enough in winter for the entire Arctic to freeze, but the ice is too thin and quickly melts in the following spring. In LIM3/1, there is no need to distribute the non-solar heat flux on several sea ice categories and the model is more stable. Compared to LIM2, LIM3/1 yields less sea ice in the Arctic but slightly more around Antarctica.

Arctic sea ice extent and thickness are displayed in Fig. 11. Most striking are the results from LIM3/5, where basically all ice disappears during summertime. Sea ice in LIM2 extends too far southwards in the North Atlantic and reaches Scandinavia, Iceland and Greenland's southern tip. With LIM3/1, the sea ice extent is more realistic, although still on the high side compared to observations. With LIM2, sea ice is much thicker than what observations suggest, with values reaching 5-6 m in the central Arctic during summer. The 2-3 m thick ice with LIM3/1 is more in line with observations. The gradient in sea ice thickness across the Arctic is modeled reasonably well with both LIM2 and LIM3/1, with the thinnest ice along the Siberian coast and the thickest ice north of the Canadian Archipelago.

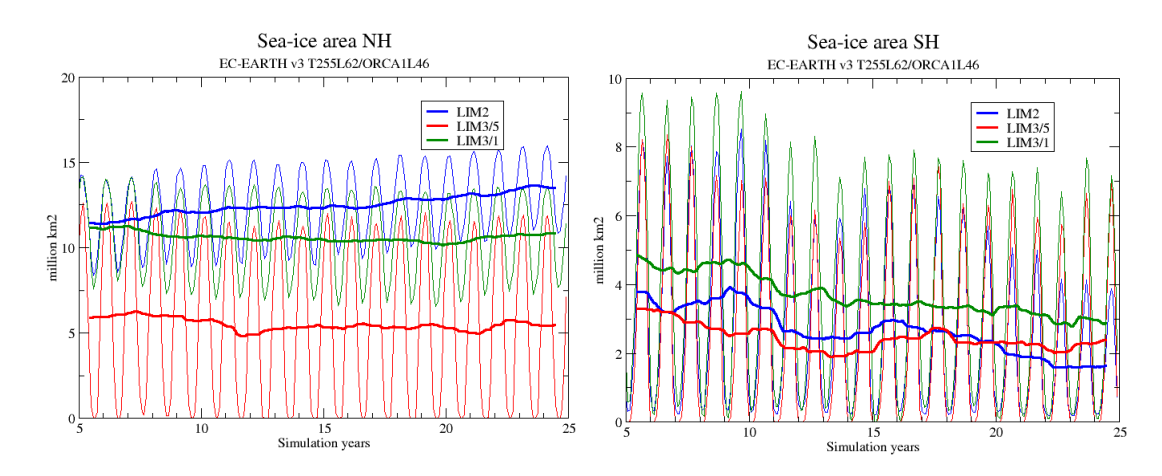


Figure 10: Sea ice area in NH (left) and SH (right). LIM3/5 denotes results from the experiment with LIM3 and 5 sea ice categories, while LIM3/1 stands for the single sea ice category LIM3 experiment with a single sea ice category. Thin lines are monthly means and thick lines 12-month running averages.

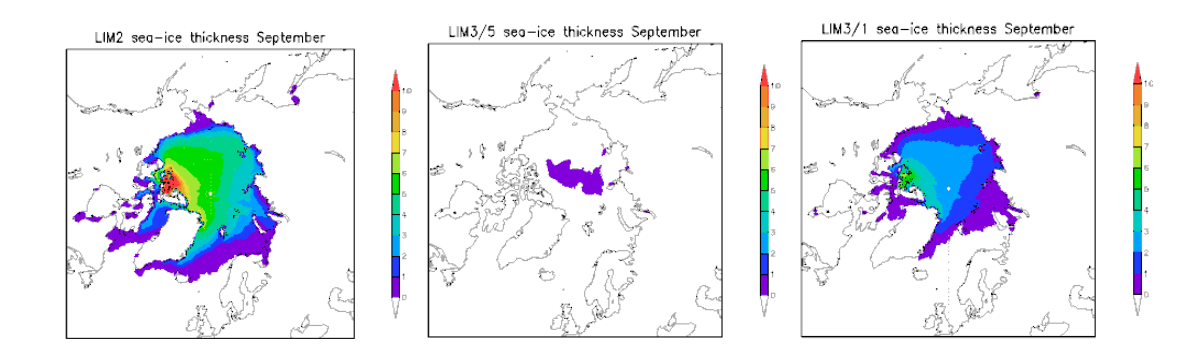


Figure 11: 20-year average of sea ice thickness (m) in the Arctic, at the time of minimum sea ice extent.

The summer Antarctic sea ice extent is too small in all model configurations, with large stretches of the Antarctic coast being ice free (Fig. 12). Most sea ice is retained with LIM2, while LIM3/5 is basically ice free. The sea ice recovers in austral winter (see Fig. 10), but remains thin. The shortcomings in the modeled sea ice in the SH are partly caused by a warm bias in the Southern Ocean, which is a known problem of NEMO.

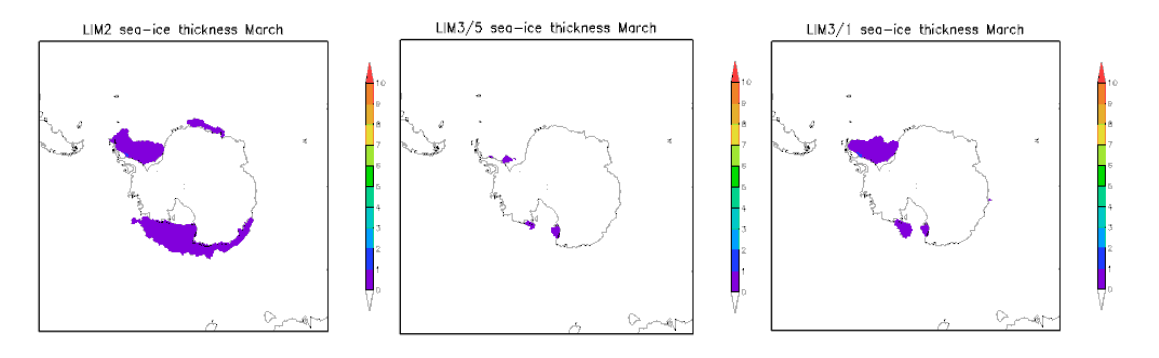


Figure 12: As Fig. 11, but for the minimum sea ice extent in the SH.

4.1.3 Preliminary conclusions

The integration of LIM3 in EC-EARTH has made some progress during the last months. LIM3 with a single sea ice category shows promising results in simulations of the present-day climate. In the Arctic, LIM3/1 has less ice — both extent and thickness — than the older LIM2 and looks more realistic. In the SH, all model configurations do not yield enough sea ice because the Southern Ocean is too warm.

The coupling of multiple sea ice categories to the atmosphere has not been solved satisfactorily yet. In the long run, the atmospheric model IFS will include multiple sea ice categories and the coupling between atmosphere and sea ice will be straightforward. On shorter term, it is planned to test the newly developed parameterization of UCL that distributes the non-solar heat flux among the different sea ice categories (see Section 3.3).

4.2 Introduction of a melt pond scheme into EC-EARTH

In parallel to the development of the next version of EC-EARTH with LIM3 as sea ice component, we have included a melt pond scheme in the older EC-EARTH version that has been used for COMBINE Stream 1 experiments and will be used for Stream 2 experiments. The global coupled model EC-EARTH v2.1 consists of IFS cycle 31r1 and NEMO2.0 with LIM2.

In EC-EARTH v2.1, the summer sea ice albedo in the Arctic is much too high compared to satellite observations (e.g., Laine 2004). Sea ice thickness in EC-EARTH seems to be overestimated in the Arctic, particularly in summer, compared to available observations and estimates (e.g., Belchansky et al., 2008). This is most pronounced along the Siberian coast, where sea ice is about 2 m thicker than estimates and leads to too much sea ice at the Siberian coast in summer. A more detailed evaluation of EC-EARTH sea ice performance is presented in Sterl et al. (2012) and Hazeleger et al. (2012).

To improve the summer sea ice albedo, a melt pond formulation has been implemented in the albedo scheme of LIM2. The new sea ice albedo parameterization is based on the existing sea ice albedo formulation in EC-EARTH v2.1/2.2 and the melt pond parameterization of Koltzow (2007):

- Melt pond fraction = $0.11 \times (2 + T_s)$ for $T_s > -2^{\circ}C$
- Albedo of melt ponds = $0.36 0.1 \times (2 + T_s)$

where T_s is the surface temperature.

4.2.1 Experiments

A 80-year long, present-day simulation (using year 2000 greenhouse gas conditions) with the new parameterization has been performed (MELT). It was started from year 250 of a simulation using EC-EARTH without melt ponds (CTRL). After 30 years, sea ice in MELT did not show trends any longer. Thus, results of year 31-80 of MELT were compared to the results of the corresponding years of CTRL (years 281-330) and observations/reanalyses.

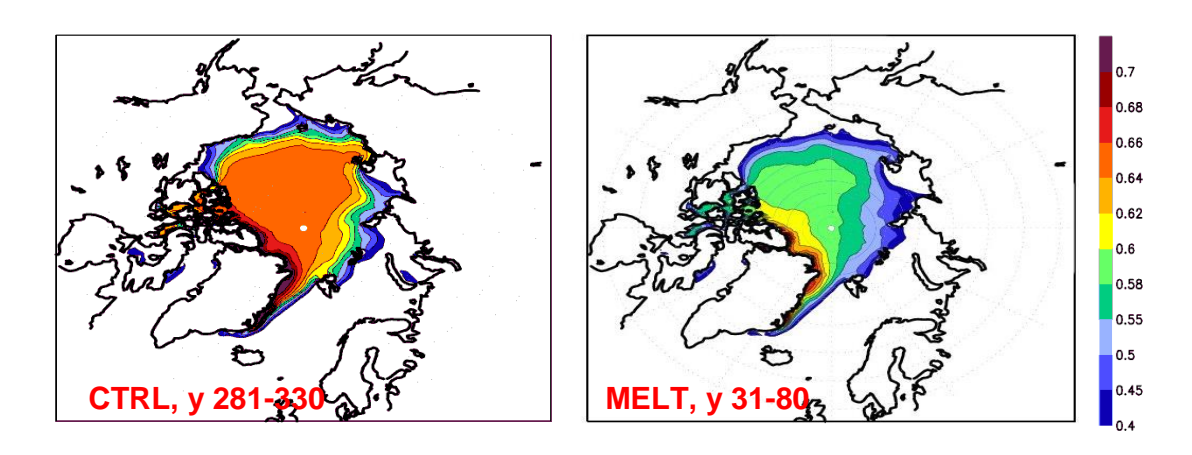


Figure 13: Summer (JJA) sea ice albedo in CTRL and MELT.

The summer sea ice albedo is substantially reduced in MELT. In the central Arctic, the decrease amounts to 0.06 (Fig. 13). As a result, the summer sea ice albedo in MELT fits much better satellite observations.

Sea ice thickness in the central Arctic varies between 2 and 3 m in March and 1-2 m in September in MELT (Fig. 14). The thickest ice is observed north of Greenland and the Canadian Archipelago, with up to 5 m. Compared to CTRL, the ice thickness is reduced by 0.6 to 1 m in the central Arctic in March and 1 to 1.5 m in September. Still, the sea ice thickness along the Siberian coast seems to be somewhat overestimated. Ice thickness in the Atlantic Arctic sector might be slightly underestimated now.

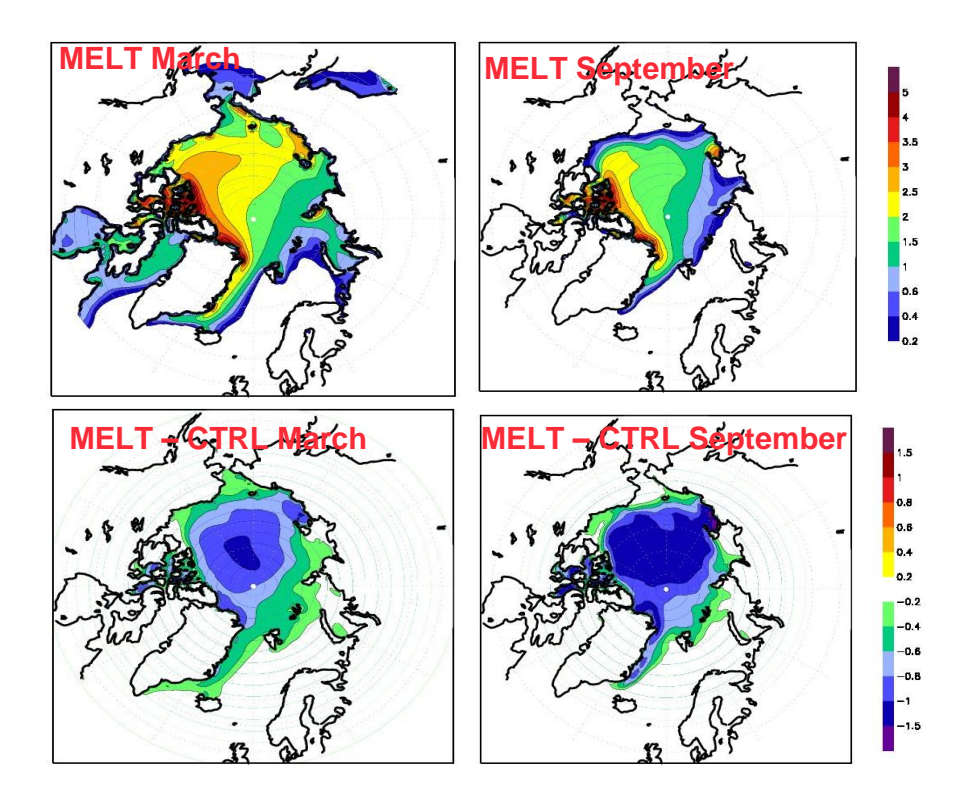


Figure 14: Sea ice thicknesses (m) in MELT in March and September (upper) and differences between MELT and CTRL (lower).

Sea ice concentration is improved in the NH in MELT. Fig. 15 shows a decrease in ice concentration along the ice edge in MELT. However, still the ice extends slightly too far southwards in the Greenland and Labrador Seas. In September, the largest reduction in sea ice concentration occurs along the Siberian coast, which leads to much more realistic ice concentrations there. The Siberian coast in MELT is almost ice free in September. Sea ice concentration in the central Arctic, particularly in the Atlantic sector, is somewhat smaller than in satellite observations.

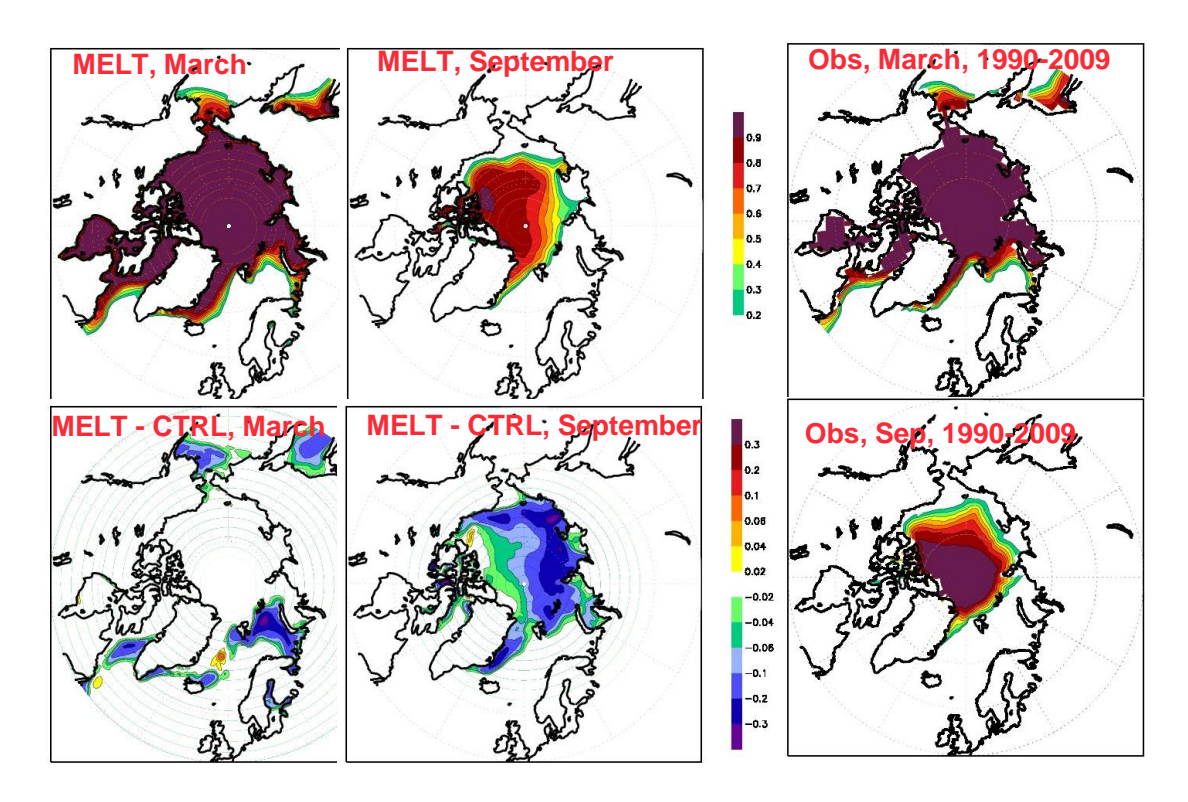


Figure 15: Arctic sea ice concentrations in MELT and in satellite observations for March and September, and differences between MELT and CTRL.

The decrease in sea ice thickness in the Arctic yields a reduced sea ice export through Fram Strait, which is overestimated in CTRL, and a weakened ice export variability. However, this is not leading to a significant improvement of the too weak deep water convection in the Labrador Sea in CTRL. The mean MOC stays at a low value, but the long-term variability is reduced probably because of the decreased freshwater export variability through Fram Strait (e.g., Holland et al., 2001).

In the SH, the implementation of the melt pond scheme impacts only slightly sea ice. CTRL is already substantially too warm in the Southern Ocean and sea ice almost totally disappears during the southern summer. Only in the Weddell Sea, multiyear ice exists, which becomes slightly thinner in MELT.

The changes in the local sea ice conditions also affect the large-scale climate. Fig. 16 shows the changes in annual mean sea level pressure (SLP) and surface air temperature (SAT) between MELT and CTRL. The changes in SLP are small, but we see an overall decrease over most of the Arctic and the North Pacific, probably due to decreased sea ice thicknesses and related increase in surface heat flux. Slightly increased SLPs are noticed over most mid- and high northern latitudes and over the

north-eastern North Atlantic. Around Antarctica, the changes in SLP are rather small. The SAT is increased by about 1°C in most of the Arctic (up to 2°C in the Barents Sea). This leads to a reduction of the cold bias present in the Arctic in CTRL. In the Weddell Sea, the SAT is enhanced by about 1°C, which increases the existing warm bias there.

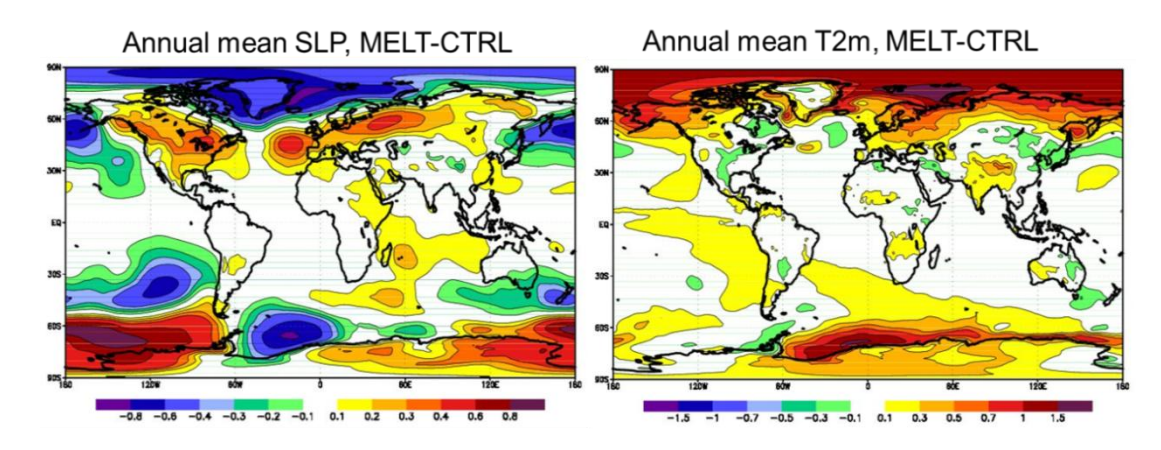


Figure 16: Differences in annual mean SLP (left; hPa) and SAT (right; °C) between MELT and CTRL.

5. Conclusion

The sea ice representation has been improved in three models: LIM2, LIM3 and GELATO. In EC-Earth-LIM2, a parameterization of melt ponds has been shown to affect the climate at large scale, including change in sea level pressure and surface air temperature. In GELATO, salt/freshwater conservation has been improved, and a parameterization of the effect of melt ponds on the sea ice albedo has been implemented and its effects have been analyzed in coupled mode. In LIM3, the representation of snow physics and of wave-ice interactions has been improved. Those new physics in LIM3 and GELATO all affect the large-scale seasonality of the ice extent and volume, with potential impact on climate and sea ice projections that should be further evaluated.

Work has also been done to improve the atmosphere-ice coupling for multi-category sea ice models. A flux distributor has been shown to properly represent the behavior of multi-category models, while exchanging only category-averaged fields, providing a coupling solution for atmospheric models which cannot "see" the ice thickness categories. This flux distributor should help to sustain a summer ice cover in EC-EARTH and IPSL-CM5 when coupled with LIM3.

While some progress has been made, substantial work remains to be done in order to achieve better sea ice simulations, in particular using multi-category models, for EC-EARTH and IPSL-CM5. However, we have good hope that the proposed flux distributor will provide a feasible solution, as the results presented here, despite preliminary, are very promising.

References

- Belchansky G.I., Douglas D.C., Platonov N.G.: Fluctuating Arctic sea ice thickness changes estimates by an in-situ learned and empirically forces neural network model, Journal of Climate, 21:716-729, doi:10.1175/2007JCI1787.1, 2008.
- Dai, M., H. H. Shen, S. F. Ackley, and M. Ikeda: Effects of pancake rafting under ocean waves on sea ice area and volume through a category transfer function, (unpublished manuscript).
- Ebert, E. and J. Curry: An intermediate one-dimensional thermodynamic sea ice model for investigating ice-atmosphere interactions, Journal of Geophysical Research, 98, 1993.
- EUMETSAT OSISAF: Global sea ice concentration reprocessing dataset 1978-2007 (v1), http://osisaf.met.no, 2010.
- Fichefet, T., Morales Maqueda, M.A.: Sensitivity of a global sea ice model to the treatment of ice thermodynamics and dynamics, Journal of Geophysical Research 102, 12609–12646, 1997.
- Hazeleger W., Wang X., Severijns C., Stefanescu S., Bintanja R., Sterl A., Wyser K., Semmler T., Yang S., van den Hurk B., van Noije T., van der Linden E., van der Wiel K.: EC-EarthV2: description and validation of a new seamless Earth system prediction model, Climate Dynamics, doi:10.1007/s00382-011-1228-5,2012.
- Holland, M., D. Bailey and B. Briegleb: Improved sea ice shortwave radiation physics in CCSM4: The impact of melt ponds and black carbon, Journal of Climate, in press, 2011.
- Holland M.M., Bitz C.M., Eby M., Weaver A.J.: The role of ice –ocean interactions in the variability of the North Atlantic thermohaline circulation, Journal of Climate, 14:656-675, 2001.
- Koltzow M.: The effect of a new snow and sea ice albedo scheme on regional climate model simulations, Journal of Geophysical Research, 112, DO7110, doi:10.1029/2006JD007693, 2007.
- Laine V.: Arctic sea ice regional albedo variability and trends, 1982-1998, Journal of Geophysical Research, 109, C06027, doi:10.1029/2003JC001818, 2004.
- Lecomte, O., Fichefet, T., Vancoppenolle, M., Nicolaus, M.: A new snow thermodynamic scheme for large scale sea-ice models, Annals of Glaciology 52(57), 337-346, 2011.
- Lüpkes, C., T. Vihma, E. Jakobson, G. König-Langlo and A. Tetzlaff: Meteorological observations from ship cruises during summer to the central Arctic: A comparison with reanalysis data, Geophysical Research Letters, 37, 2010.
- Madec, G.: NEMO reference manual, ocean dynamics component: NEMO-OPA. Note du Pole de modélisation, Institut Pierre-Simon Laplace (IPSL), France, No. 27 ISSN No. 1288-1619, 2008. Available from: http://www.lodyc.jussieu.fr/NEMO/general/manual/NEMO_book.pdf.
- Massonnet F., Fichefet T., Goosse H., Vancoppenolle M., Mathiot P., and König C.: On the influence of model physics on simulations of Arctic and Antarctic sea ice, The Cryosphere, 5, 687-699, 2011.
- Maykut, G.A.: The surface heat and mass balance, In: Untersteiner, N. (Ed.), The Geophysics of Sea Ice, NATO ASI Series B: Physics, vol. 146, Plenum Press, New York, pp, 395-464, 1986.
- Maykut, G.A. and Untersteiner, N.: Some results from a time-dependent thermodynamic model of sea ice, Journal of Geophysical Research 76, 1550-1575, 1971.

- Schmidt, G.A., C.M. Bitz, U. Mikolajewicz and L.-B. Tremblay: Ice-ocean boundary conditions for coupled models, Ocean Modelling, 7, 59-74, doi:10.1016/S1463-5003(03)00030-1, 2004.
- Sterl, A., and S. Caires: Climatology, variability and extrema of ocean waves: The web-based knmi/era-40 wave atlas, International Journal of Climatology, 25, 963-977, 2005.
- Sterl A., Bintanja R., Brodeau L., Gleeson E., Koenigk T., Schmith T., Semmler T., Severijns C., Wyser K., Yang S.: A look at the ocean in the EC-Earth climate model, Climate Dynamics, doi:10.1007/s00382-011-1239-2, 2012.
- Thorndike, A.S., Rothrock, D.A., Maykut, G.A., Colony, R.: The thickness distribution of sea ice, Journal of Geophysical Research 80, 4501-4513, 1975.
- Vancoppenolle, M., T. Fichefet, H. Goosse, S. Bouillon, G. Madec and M.A. Morales Maqueda: Simulating the mass balance and salinity of Arctic and Antarctic sea ice. 1. Model description and validation, Ocean Modelling, 27, 33-53, doi:10.1016/j.ocemod.2008.10.005, 2009.
- Voldoire, A., E. Sanchez-Gomez, D. Salas y Mélia, B. Decharme, C. Cassou, S.Sénési, S. Valcke, I. Beau, A. Alias, M. Chevallier, M. Déqué, J. Deshayes, H. Douville, E. Fernandez, G. Madec, E. Maisonnave, M.-P. Moine, S. Planton, D.Saint-Martin, S. Szopa, S. Tyteca, R. Alkama, S. Belamari, A. Braun, L. Coquart, F. Chauvin.: The CNRM-CM5.1 global climate model: description and basic evaluation, Climate Dynamics, DOI:10.1007/s00382-011-1259-y, 2012.